Phase of the transmission amplitude for a quantum dot embedded in the arm of an electronic Mach-Zehnder interferometer

L. V. Litvin, A. Helzel, H.-P. Tranitz, W. Wegscheider, and C. Strunk
Institut für Experimentelle und Angewandte Physik, Universität Regensburg, D-93040 Regensburg, Germany
(Received 4 December 2009; revised manuscript received 23 February 2010; published 18 May 2010)

We investigate an electronic Mach-Zehnder interferometer with high visibility in the quantum Hall regime. The superposition of the electrostatic potentials from a quantum point contact (QPC) and the residual disorder potential from doping impurities frequently results in the formation of inadvertent quantum dots (QDs) in one arm of the interferometer. This gives rise to resonances in the QPC transmission characteristics. While crossing the QD resonance in energy, the interferometer gains a phase shift of π in the interference pattern.

DOI: 10.1103/PhysRevB.81.205425 PACS number(s): 73.23.Ad, 73.63.Nm

I. INTRODUCTION

The conductance G of an Aharonov-Bohm (AB) ring oscillates with magnetic field B with a period ΔB determined by the area A between two interfering paths $\Delta B=\Phi_0/A$, where $\Phi_0=h/e$ is the flux quantum. The combination of the AB ring with a quantum dot (QD) in one of its arms gives the opportunity to measure the phase of transmission amplitude through the QD.[1] The dot, tuned to a transmission resonance, sustains coherent transport all over the width of the resonance peak. So far this was realized in different groups by recording AB oscillations as a function of the magnetic field and tracing their phase with respect to the energy of the resonant state, which was controlled by a plunger gate.[2–4] Fano resonances were observed in Ref. 4 while other works[2,3] show the phase evolution of AB oscillations while scanning through each Coulomb peak in energy changing the plunger gate. Here a slip by π was seen, what can be explained in a single-particle picture. For the observed π jump between two Coulomb peaks,[2] a theory involving many particles is needed. Besides the phase of the transmitted current also the phase of the reflected current was probed,[3] which showed similar results. In order to determine the energy dependence of the phase, it was necessary to record many $G(B)$ traces differing in plunger gate, each resulting, in a single point in the phase evolution. The question arises, whether one could directly measure the phase in an interferometer, when the QD crosses a resonance. This has two attractive advantages. First, the measurement process speeds up because information about phase is acquired in a single sweep of the plunger gate. Second, with such a fast measurement process, one could think about detection of the charge state for the QD by measuring its transmission (reflection) phase. The latter can be important for building charge qubits based on double quantum-dot system. However, in conventional AB interferometers, the small interference contrast (typically 10%) and signal noise makes this task difficult.[4] In this work, we report on measurements of QD transmission phase with an electronic Mach-Zehnder interferometer (MZI).[5] The electronic Mach-Zehnder interferometer employs edge channels of a two-dimensional (2D) electron system in the quantum Hall regime and quantum point contacts as beam splitters. The interference contrast can be very large, up to 80 %, at temperatures near 20 mK.[6]

II. EXPERIMENTAL DETAILS

The interferometer (see Fig. 1) was fabricated on the basis of a modulation-doped $GaAs/Ga_xAl_{1-x}As$ heterostructure containing a 2D electron gas (2DEG) 90 nm below the surface. At 4 K, the unpatterned 2DEG density and mobility were $n=2.0\times10^{15}$ m^{-2} and $\mu=206$ $m^2/(V\,s)$, respectively. The details of fabrication procedure can be found in Ref. 7. Each arm of the MZI was approximately 9 μm long and the gap between the tips of quantum point contacts was 400 nm. This interferometer showed a maximum visibility of 56% and an area of 25 μm^2 between interfering paths, found from the period of Aharonov-Bohm oscillations. A standard lock-in technique ($f\sim300$ Hz) with 1 μV excitation at terminal S and detection at terminal D2 was employed (see Fig. 1). All measurements were performed at a temperature below 50 mK.

III. CHARACTERIZATION OF THE QUANTUM POINT CONTACTS

In many experiments, the transmission characteristics of the QPCs, in high perpendicular magnetic field exhibit resonances superimposed on the conductance steps [Fig. 2(a), see also Refs. 8–10]. As we will show below, our data suggest that this originates from the Coulomb blockade of a quantum dot formed inadvertently by the disorder potential in the vicinity of the QPCs. The interference contrast was highest for the outer edge channel. To record the characteristics in Fig.

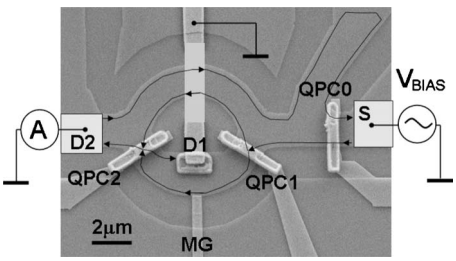

FIG. 1. Scanning electron microscopy image of Mach-Zehnder interferometer with the scheme of paths for nonequilibrium current. The transmission of QPC1 and QPC2 is set to 0.5. QPC0 transmits the outer edge channel and reflects the inner one in case the filling factor being more than 1. The MG is used to shift the phase.

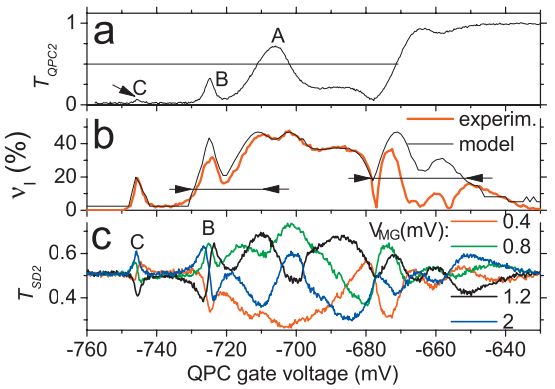

FIG. 2. (Color) (a) Transmission characteristic of QPC2 as a function of the QPCs gate voltages at $B=4.8$ T. The horizontal line denotes half transmission of the QPC which should in a single-particle picture correspond to the highest visibility. (b) Visibility of Aharonov-Bohm oscillations, experimentally measured (thick red line) and calculated from transmission of QPC2 (thin black line) versus QPC2 gate voltage [$T_{QPC1}=0.5$, see Eq. (2)]. The regions of discrepancy are marked by arrows. (c) Interferometer current for different modulation gate voltages, i.e., different AB phases ($T_{QPC1}=0.5$).

2(a), (i) the magnetic field was set to 4.8 T (filling factor 1.6), (ii) QPC0 was adjusted to transmit only the outermost channel, and (iii) the gate voltage for QPC2 was swept to negative voltages while keeping QPC1 open [see also Fig. 3(a)]. A sequence of peaks [marked by letters A, B, and C in Fig. 2(a)] in the gate characteristics of QPC2 appears at transmissions less than 1. It is of interest to check if any peak structure can be found in the dependence on a magnetic field. The magnetic field dependence of transmission of QPC2 is plotted in Fig. 3(c). While sweeping the magnetic field, the data was recorded after adjusting QPC0 to reflect the half-filled upper Landau level, opening QPC1, and tuning the gate voltage of QPC2 at the maximum of peak "A" (T_{QPC2} $=0.65$)($B=4.8$ T). The overall QPC2 transmission in Fig. 3(c) decreases nonmonotonically from left to right. Increasing magnetic field changes energies of the Landau levels. For low magnetic fields ($B<3.8$ T), QPC2 is fully transmitting the corresponding edge channel whereas for high magnetic fields ($B>6.4$ T), it is mostly reflecting it. Also QPC0 can do this but while $T_{QPC0}=1$ at $B=4.8$ T, $T_{QPC2}=0.65$ as mentioned above, i.e., the potential barrier of QPC2 is higher than of QPC0. Additionally we find oscillatory components in the QPC2 transmission, which are not expected for a single barrier but could easily appear in a device with two and more barriers or an antidot structure.[11] Fourier analysis reveals two frequencies in B, corresponding to periods of 0.27 and 0.18 T, and their higher harmonics. When interpreted as Aharonov-Bohm oscillations ($\Delta B \cdot A = e/h$), these two periods correspond to areas enclosed by circumference with diameter $d=2\sqrt{A/\pi}$ of 140 and 170 nm. This is well compatible with the lithographic gap between QPC tips (400 nm) and with the spatial variation in the disorder potential near 100 nm measured, e.g., in Ref. 12 for 2DEG structure with parameters similar to ours. Aharonov-Bohm oscillations induced by potential fluctuations in single QPC in high magnetic field was reported before.[13] In addition, we found that the resonances in Fig. 2(a) are also dependent on cooling cycle, i.e., the shape of the resonances is unique for each cool down. This indicates that charging of donor atoms in the doping layer plays a role in the resonance formation.

We conclude that, due to the background potential near or in between the QPC tips, electrons are localized leading to discrete energy levels. This was found by several groups but yet without a clear explanation so far. As we will describe in the next paragraph, this influences the transport properties of the MZI.

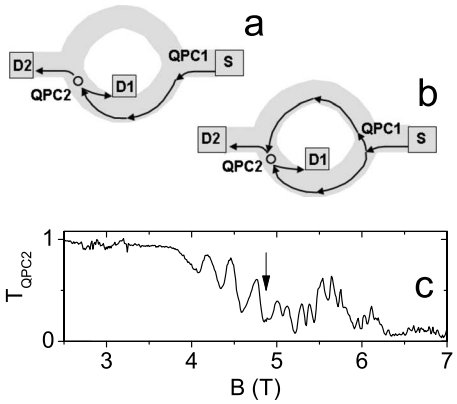

FIG. 3. (a) Scheme for probing transmission characteristic of QPC2 with QPC1 opened, and that (b) for interference experiment with both QPCs partially transmitted. The circle at the QPC2 symbolizes the quasibound state of quantum dot. (c) Oscillatory transmission of outermost edge channel as a function of magnetic field when transmission of QPC2 is less than 1. The arrow marks the point where the additional frequency (with almost half period) sets in.

IV. PHASE SHIFTS BY THE QUANTUM DOT

Next, we discuss the response of the MZI interference near the resonances in the transmission of QPC2. To investigate this, first, the QPC1 must be set to half transmission, generating two interfering paths as shown in Fig. 3(b). Second, the interference signal must be measured as a function of the QPC2 gate voltage. Here two possibilities arise depending on the regime for a modulation gate (MG) voltage V_{MG} which is normally used to observe interference by shifting the phase of one arm with respect to other. These are (i) sweeping V_{MG} simultaneously with the QPC2 gate voltage and (ii) keeping V_{MG} constant. The former allows to determine the interference contrast as a function of V_{QPC2} (or T_{QPC2}) and was demonstrated before [Ref. 10, Fig. 1(c); Fig. 2(a)]. In contrast, the latter is sensitive to any phase gain during a change in the QPC2 gate voltage. We explore both of these opportunities starting from the measurement of the span for AB oscillation vs V_{QPC2}. The relative amplitude of oscillations is called visibility ν_I, $\nu_I=(I_{max}-I_{min})/(I_{max}+I_{min})$, and is plotted in Fig. 2(b). Here one sees that the visibility ν_I peaks at the transmission resonances A, "B," and "C." Qualitatively, this is explained by the fact that the visibility has a maximum when both arms carry equal current, i.e., at $T_{QPC}=1/2$ (a quantitative analysis follows below).

Therefore, the closer T_{QPC} is to 1/2, the higher is the visibility. The phase information does not show itself in this experiment but it does when the modulation gate voltage V_{MG} is kept constant [Fig. 2(c)]. We focus on the resonances B and C where an abrupt change in the current is observed. Some traces show at B and C a clear alternation between a peak and a dip structure. That means if the AB oscillations are adjusted to a maximum with MG, it changes abruptly to a minimum, when passing the resonance. This implies a phase change by π at the resonance. Such phase shift in connection with resonant behavior was already noticed before but the physical origin of the resonances remained unclear.[14]

Now we address quantitatively the results in Fig. 2 in the framework of a model assuming noninteracting particles. This model predicts the MZI transmission coefficient,[5]

$$T_{SD2} = |t_1 r_2|^2 + |r_1 t_2|^2 - 2|t_1 t_2 r_1 r_2| \cos \Delta\varphi, \tag{1}$$

here t_i, r_i are transmission and reflection amplitudes of QPCs and $\Delta\varphi$ is the phase difference between the interferometer arms. From this formula, one can easily find the expression for the visibility as a function of one of the QPC transmission, namely,

$$\nu_I = z \cdot 2\sqrt{T_{\mathrm{QPC2}}(1 - T_{\mathrm{QPC2}})}, \tag{2}$$

where the factor $z<1$ accounts for the decoherence at finite temperature. We have used $z=0.42$ corresponding to the maximum measured visibility. Using this expression and the measured transmission values for T_{QPC2} in Fig. 2(a), we calculate the dependence of visibility $\nu_I(T_{\mathrm{QPC2}})$ and compare it with the experimental one. The black, thin line in Fig. 2(b) shows the result, which agrees in general well with the experiment. There are two regions of deviation from the simple model of Eq. (2), marked by arrows in Fig. 2(b), and peak B is within one of those. In contrast to this the peak C, with small transmission value, is well described by the model, as well as the region with transmission close to 1 ($V_{\mathrm{QPC2}} > -651$ mV) and the one on the right wing of the peak A ($-708 < V_{\mathrm{QPC2}} < -678$ mV).

Following the noninteracting particle approach from Ref. 2, we add a quantum dot to the above-mentioned MZI, whose transmission properties are modeled by the Breit-Wigner formula. We replace transmission and reflection amplitudes of QPC2 by those of the quantum dot. The dot transmission amplitude has a phase which must be added to the cosine argument in Eq. (1). Then the coherent component in MZI transmission is proportional to $T_{SD2coh} \propto |t_{\mathrm{QD}}||r_{\mathrm{QD}}|\cos[\Delta\varphi + \theta(t_{\mathrm{QD}})]$, where t_{QD}, r_{QD}, and $\theta(t_{\mathrm{QD}})$ stand for the transmission (reflection) amplitude of QD and the phase of QD, respectively. The Breit-Wigner formula for the selected state with the energy E_n,

$$t_{\mathrm{QD}} = |t_{\mathrm{QD}}| e^{i\theta} = \frac{(i\Gamma/2)}{(E - E_n + i\Gamma/2)} \tag{3}$$

with $\theta(t_{\mathrm{QD}}) = \arctan[\frac{2}{\Gamma}(E - E_n)]$ and relation $|r_{\mathrm{QD}}| = \sqrt{1 - |t_{\mathrm{QD}}|^2}$ were applied for the simulation of experimental curves [in Fig. 4].

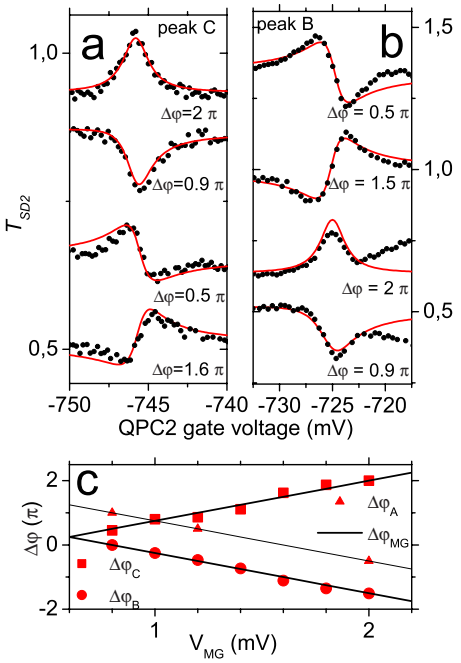

FIG. 4. (Color online) (a) The resonance C (dots), shown in Fig. 2(c), fitted by model of an interferometer with quantum dot in one arm (full line) for different voltages of modulation gate $V_{\mathrm{MG}}=0.4$, 0.8, 1.2, and 2.0 mV changing from bottom to top. (b) The same for the peak B in Fig. 2(c). The curves in (a) and (b) shifted for clarity except lowest one. (c) The phase shift between interferometer arms, found from the fit to the resonances B and C, plotted as a function of V_{MG}. The full lines in (c) are expected slopes resulted from AB period $\Delta V_{\mathrm{MG}}=1.6$ mV in V_{MG}. The phase evolution for the resonance A was evaluated by procedure described in the text.

This model rather well describes the interference resonances B and C. The peak A was analyzed below only qualitatively because it deviates over a wide range from Eq. (3). The resonance C was matched well by calculated curves [Fig. 4(a)] with resonance width of $\Gamma_C=1.9$ mV determined from fit by Lorentzian, the peak in the QPC2 transmission in Fig. 2(a). Therefore, the only fitting parameter for this interference resonance was the phase shift $\Delta\varphi$. For peak B [Fig. 4(b)], an effective transmission resonance, of smaller amplitude and width [$\Gamma_B=2.5$ mV instead 3.4 mV in Fig. 2(a)], matching the experimental visibility in Fig. 2(b), was used.

In addition to the good matching of the experimental curves in Figs. 4(a) and 4(b) to Eq. (3), the validity of our interpretation is supported by the correlation between the phase set by the modulation gate voltage and that determined from the best fit to experimental data in Figs. 4(a) and 4(b) with Eq. (3). The period of AB oscillations in V_{MG} was found to be 1.6 mV, which corresponds to phase change of 2 π. In Fig. 4(c), we plot the phase found from fitting as a function of modulation gate voltage $\Delta\varphi(V_{\mathrm{MG}})$ for the peaks C (squares) and B (circles), and from these graphs extract the slope a of $\Delta\varphi = aV_{\mathrm{MG}}$. We find $\Delta\varphi = \pm 2\pi/1.6$ mV, which is in perfect agreement with the period V_{MG} extracted from the interference pattern $I_{D2}(V_{\mathrm{MG}})$.

The phase shift $\Delta\varphi$ of peak A can only be determined qualitatively as mentioned above. From Figs. 4(a) and 4(b), one can see that a peak in the interference resonance corre-

sponds to $\Delta\varphi=2\pi$, the dip to π, combination left peak/right dip to $\pi/2$, and left dip/right peak to $3\pi/2$. Comparing this with the shape of the interference resonance of peak A, we can deduce an approximate phase shift. It is interesting to investigate the direction of the phase evolution in Fig. 4(c) $\Delta\varphi(V_{\mathrm{MG}})$ for the neighboring peaks A and B, and peak C.

As a result, peak A shows the same direction of phase evolution as B [Fig. 4(c), triangles]. On the other hand, the phase evolution of peak C goes into the opposite direction. This discrepancy may originate from the variability of two barriers since the dot is defined by the single QPC2 gate and the disorder potential. Tuning the gate potential of QPC2 changes simultaneously the two barrier heights of the QD and its well depth.

The largest of the two barriers must be the branching point of the interferometer path. If the barriers interchange their height, the branching point will interchange its location as well. In this case, the π phase shift from the quantum dot may contribute either to the upper arm or to the lower one [Fig. 3(b)], and depending on this, gain its different sign in the paths phase difference.

V. CONCLUSIONS

In summary, we have shown that the frequently observed transmission resonances in quantum point contacts within an electronic Mach-Zehnder interferometer stem from inadvertent quantum dots formed by the disorder potential in high magnetic field and measured the phase of the transmission amplitude through a quantum dot. We propose to utilize this effect for the detection of the state of charge qubits in the vicinity of a Mach-Zehnder interferometer via their reflection phase. Such a dispersive readout may allow more sensitive and less invasive detection than the currently used quantum point contacts.

ACKNOWLEDGMENTS

We are grateful to K. Kang, K. Kobayashi, S. Ludwig, and T. Hecht for fruitful discussions. The work was funded by the DFG within the SFB631 "Solid state quantum information processing" and the BMBF via project 01BM465 within the program "Nanoquit."

[1] A. Yacoby, M. Heiblum, D. Mahalu, and H. Shtrikman, Phys. Rev. Lett. **74**, 4047 (1995).
[2] R. Schuster, E. Buks, M. Heiblum, D. Mahalu, V. Umansky, and H. Shtrikman, Nature (London) **385**, 417 (1997).
[3] E. Buks, R. Schuster, M. Heiblum, D. Mahalu, V. Umansky, and H. Shtrikman, Phys. Rev. Lett. **77**, 4664 (1996).
[4] K. Kobayashi, H. Aikawa, S. Katsumoto, and Y. Iye, Phys. Rev. Lett. **88**, 256806 (2002).
[5] Y. Ji, Y. Chung, D. Sprinzak, M. Heiblum, D. Mahalu, and H. Shtrikman, Nature (London) **422**, 415 (2003).
[6] I. Neder, N. Ofek, Y. Chung, M. Heiblum, D. Mahalu, and V. Umansky, Nature (London) **448**, 333 (2007).
[7] L. V. Litvin, A. Helzel, H.-P. Tranitz, W. Wegscheider, and C. Strunk, Phys. Rev. B **78**, 075303 (2008).
[8] I. Neder, F. Marquardt, M. Heiblum, D. Mahalu, and V. Umansky, Nat. Phys. **3**, 534 (2007).
[9] P. Roulleau, F. Portier, D.C. Glattli, P. Roche, A. Cavanna, G. Faini, U. Gennser, and D. Mailly, Phys. Rev. B **76**, 161309(R) (2007).
[10] L. V. Litvin, A. Helzel, H.-P. Tranitz, W. Wegscheider, and C. Strunk, Physica E (Amsterdam) **40**, 1706 (2008).
[11] M. Kataoka, C. J. B. Ford, G. Faini, D. Mailly, M. Y. Simmons, and D. A. Ritchie, Phys. Rev. B **62**, R4817 (2000).
[12] G. A. Steele, R. C. Ashoori, L. N. Pfeiffer, and K. W. West, Phys. Rev. Lett. **95**, 136804 (2005).
[13] P. H. M. van Loosdrecht, C. W. J. Beenakker, H. van Houten, J. G. Williamson, B. J. van Wees, J. E. Mooij, C. T. Foxon, and J. J. Harris, Phys. Rev. B **38**, 10162 (1988).
[14] P. Roulleau, F. Portier, P. Roche, A. Cavanna, G. Faini, U. Gennser, and D. Mailly, Phys. Rev. Lett. **102**, 236802 (2009).